Master's science Thesis

Evaluation of gantry angle optimization for IMRT treatment planning systems using the Pareto front approach

Maria Thor

Supervisors: Anna Karlsson[1], Claus Behrens[1], Per Engström[2], Crister Ceberg[3] and Tommy Knöös[2]

1 Herlev University Hospital, Denmark

2 Lund University Hospital, Sweden

3 Lund University, Sweden

Contents

1. Introduction

1.1 Purpose

The aim of this study was to compare two inverse Treatment Planning Systems (TPSs); Eclipse IMRT external beam planning system Version 8.5.0 (Eclipse), Varian Medical systems, USA and Elekta's Oncentra Masterplan 3.1 SP3 (OMP), Nucletron, The Netherlands. These two systems constituted dynamic and segmented delivery technique. The comparison was carried out by using the Pareto front approach. More specifically, the purpose was to investigate IMRT with seven equally spaced beams with the most optimal seven gantry angles generated by using Gantry Angle Optimization (GAO).

The evaluation was undertaken for three head and neck (H & N) cancer cases and was based on the comparison of Pareto fronts generated by data extracted from the dose statistics in the calculated Dose Volume Histograms (DVHs). The study intended to investigate the trade-off between the average absorbed dose to the parotid gland that was overlapping with at least one of the Planning Target Volumes (PTVs) and the dose coverage of that PTV.

1.2 Background

Each day, 20 000 people die as a consequence of cancer. Cancer has become one of the most common reasons of death worldwide: it is the second most common reason of death in the industrial countries and the third most common in the less developed countries [1, 2]. Cancer has been treated using several methods. One reliable technique is external radiotherapy with photons. Delanay et al. [3] has calculated that it would be beneficial for 52 % of all the cancer patients to receive radiotherapy at some point during their illness. Beneficial for a palliative intention is synonymous with easing the pain and for a curative intention it is equal to cure the patient from the cancer. The aim with radiotherapy is to annihilate tumour structure, while keeping the absorbed dose to normal structure as low as possible. This can also be translated with achieving dose conformity in the PTV while keeping the absorbed dose to Organs at Risk (OARs) low.

According to the International Commission on Radiation Units and measurements (ICRU), heterogeneity between +7% and -5% of the prescribed dose in the PTV is acceptable [4]. One of the limits with conventional radiotherapy concerns dose conformity, especially to concave parts of the PTV that surrounds an inner sensitive structure, which in turn limits the absorbed dose. The reason for this unconformity outside the PTV is due to the unmodulted beams' lack of ability to enclose the target volume and see the 3-D shape of it from each direction [5]. Dose conformity in the PTV along with simultaneously maintenance of low dose to a certain OAR is equivalent to an increase of the therapeutic ratio (TR) [5, 6]. The TR measures how well tumour control Probability (TCP) and normal tissue complication probability (NTCP) are maintained and is defined as the separation of the TCP and NTCP.

The work by Brahme et al. [7] concerning inverse dose planning of the optimum shape of the dose distribution for each gantry position is considered as the starting-point for the present Intensity Modulated Radiation Therapy (IMRT) techniques and has brought the development of the radiotherapy to a new level [6, 8]. IMRT is an advanced method of conformal radiotherapy and permits optimal dose distribution to the target volume while preserving surrounding normal tissues [9]. The fluence in each beam is modulated by utilizing the Multi Leaf Collimators (MLCs) and can either be delivered with segmented technique i.e. the dose is only delivered while the leaves are being stationary by combining small elementary static fields [9, 10], or dynamically where the beam is on during the movement of the leaves [5].

IMRT allows sparing of critical normal structures in *e.g.* the H & N region without compromising dose to the tumour and is therefore desirable for several clinical applications and essential in some [5, 11 and 12]. Further, H & N cancer is well suited and challenging for

IMRT since it includes many OARs [13], such as the spinal cord as well as the parotid glands. Apart from this, the fact that superior target coverage compared to that of conformal radiotherapy still remains [5, 14 and 15].

1.3 Inverse dose planning

The fluences to be delivered with the technique of IMRT are created by inverse treatment planning which is an iterative process, created from the preferred dose distribution. The operator put demands on minimum and maximum dose to the PTV and dose restrictions to critical structures as well. An objective function for every structure of interest is introduced in the optimization algorithm, which makes it possible to measure the progress in reaching the desired solution [5].

In inverse treatment planning, the desired demands i.e. the objectives in a certain treatment plan are first specified to generate a set of intensity modulated fluences from which the dose distribution is calculated [16]. The main difference compared to traditional forward planning lies in these demands rather than denoting the forward planning as a trial and error process since the inverse planning also performs many trials or iterations. The capacity to distinguish the three-dimensional (3D) shape of the target volume for each desired angle of the inverse planning add up to a much more conformal dose distribution than that of the unmodulated beams in the forward planning [5] (Figure 1).
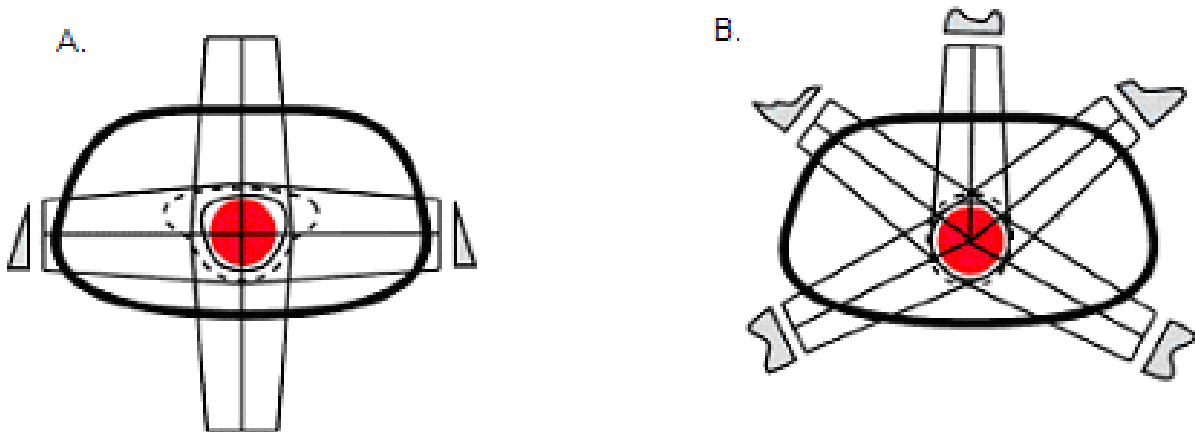
Figure 1. The figure illustrates higher dose conformity while using inverse planning (B) for a defined target compared to that of using traditional forward planning (A) *e.g.* by Courtesy of Varian Medical systems [16].

1.4 Optimization

As the optimization takes part, objective functions for every desired structure is introduced to measure how far the result is from the desired solution. Often an overall voxel-by-voxel based problem and a quadratic objective function is used [5] which includes a weighted sum of the squared difference between the desired and the actual dose. The desired dose for the ith voxel can be denoted as d_i^{des}, d_i as the actual dose and the penalty for deviating from the desired dose as s_i for N considered voxels. The objective function can then be defined by F (Eq. 1).

$$F = \sum_{i=1}^{N} s_i \left(d_i - d_i^{des} \right)^2 \qquad \text{(Eq. 1)}$$

The goal is to gradually achieve a dose distribution similar to that of the specified and desired dose distribution. In some TPSs the penalties are user-defined by type as hard or soft

constraints for the targets and structures. Moreover, the penalties work outside the specified dose goals for the target and the OAR [5].

To achieve an absorbed dose close to the specified dose distribution, the beam let weights can be changed in a deterministic manner. The gradient technique is based on the calculated changes in the beam lets and is such a minimizing process where the value of the objective function is reduced until no alteration exists [5].

1.5 Sliding windows for Dynamic Delivery (DMLC)

The purpose of the adjacent high-density attenuating MLC is to protect areas outside the PTV from irradiation in analogy with the used shielding blocks in conventional radiotherapy [5]. What is designated as Sliding windows or Dynamic MLC (DMLC) is that the opening, which is formed by the pair of opposing MLC leaves, moves over the PTV as the beam is on [5]. In DMLC, the leaves' velocity can obtain various values anywhere between 0 up to the maximum leaf speed [13].

The technique of the DMLC is dependant of the properties of the MLCs [5]. IMRT delivered with DMLC requires a conversion of the radiation intensity map into a leaf sequence which in turn controls the movement of the MLCs as the beam is on [17]. This means that the delivery might be affected of the mechanical limits and irregularities of the MLCs. When including this in the optimization chain it comes clear that the final actual dose calculation may differ from that of the desired dose [5, 16]. The limits are especially grounded on the rounded leaf ends that will result in a dose increase more than what is expected as a consequence of the leaf transmission [5].

1.6 Step and shoot for Segmented Delivery (SMLC)

Segmented delivery technique (SMLC) means that the absorbed dose only is delivered while the leaves are being stationary i.e. no dose is delivered as the leaves move to the next segment position [5]. SMLC is often referred to as an extreme case of the DMLC [5]. Hence, the leaves' velocity is either zero or that of the maximum speed which leads to a minor degree of freedom than that for the DMLC [13]. With SMLC the dose is delivered by several segments and the aim of this segmentation is to reconstruct individual fluence distributions for each beam as closely as possible by determining the properties of the MLC segments [18]. The MLC segments are limited to a number of fluence levels among the beams where each level is dissolved into smaller elements that each represents the opening for a leaf pair [18]. With a large number of levels, SMLC approaches DMLC but this requires many segments of short beam-on-times which may introduce a stability problem for some linear accelerators. The openings of each leaf-pair are organized into segments and depend on the complexity of the fluence [18]. The segments include properties like leaf position bounds, leaf over travel, minimum gaps for opposing adjacent leaves and leaf separation for adjacent leaves within each leaf bank as well [18].

A disadvantage of SMLC, when compared to DMLC, is that the intensity profile requires the desired fluence intensity profile to be approximated by discrete levels of intensity [5]. The leaf sequence is designed to deliver such a discrete profile.

1.7 Inverse dose planning in Eclipse and OMP

The inverse dose planning procedure in both Eclipse and OMP is divided into several steps. As a first step the target volume and critical structures are defined and outlined from the CT-images. This is followed by the manual deployment of the needful angles and number of fields. The lower and upper Dose Volume Objectives (DVOs) for each PTV as well as upper objectives for each OAR of concern are then defined. Lower objectives ensure that a volume receives a minimum absorbed dose [16, 18]. Any structure with a lower dose volume

objective is treated as a target [16, 18]. Upper objectives limit the absorbed dose to any structure [16, 18 and 19] and can be used to enhance dose uniformity in target volumes. All defined DVOs are weighted together and composite one objective function that is minimized during the optimization. The specified geometry concludes the degree of dependence between the objective functions during the optimization procedure [19].

In Eclipse, the DVOs, and their importance as well, are possible to alter during the entire optimization until the prescribed dose objectives of the treatment plan are satisfied. The iterations can be interrupted at any time during the optimization process, or can be left to terminate on its own [16]. In OMP, the final importance is defined in advance along with a stop criterion that commands the optimization process to stop after a defined number of iterations [19].

The fluences in Eclipse are generated in two steps; the optimal fluences and the actual fluences. The optimal fluences are an ideal modulation of the fields with lack of respect to physical and mechanical limits of the MLCs [16, 18]. The optimal fluences are created by adjusting the ray weights using a gradient optimization where each beam is divided into elementary pencil beams and its dose contribution to the voxels in the target and critical organs are calculated. As the optimal fluences are impossible to deliver, the conversion to an actual fluence is necessary [16]. In Eclipse, the actual fluences include the limitations of the leaf motions which are calculated through the Leaf Motion Calculator (LMC). This is an iterative process where the actual fluence is estimated from the DMLC sequence until suited agreement between the actual fluence and optimal fluence is achieved. To create a 3D absorbed dose distribution for further evaluation, the final dose calculation might be accomplished with the algorithm of Pencil Beam Convolution Version 8.1.14 (PBC) [16, 18].

The sparing of the normal tissues in the inverse treatment planning is considered different in the TPSs. In Eclipse, a Normal Tissue Objective Parameter (NTOP) can be implicated into the optimization. This especially prevents hot spots in the normal tissues and result in a sharp dose gradient around the targets [16]. The shape of the NTOP is calculated as a function of the distance from the target border. A priority on the NTOP determines the relative importance of the normal tissue objective in relation to other optimization objectives and is similar to that in the dose volume objectives. The NTOP is calculated for all body voxels. If the plan contains several targets, the NTOP for a specific body point is calculated from all targets, and the highest one is used in the optimization. Apart from the dosimetric properties of the plan, the X- and Y fluence priorities of the smoothing objective function are defined. These make it particularly possible to achieve more deliverable DMLC sequences [16]. The degree of the modulation of the fluence intensity is always reduced when fluence smoothing is applied [16]. Smoothing in the X-direction affects the separation between the two MLC banks and smoothing in the Y-direction helps minimize tongue and groove effects since it synchronises each bank's MLCs.

OMP uses Direct Step-and-Shoot (Direct S & S) delivery. Direct denotes that the settings for the MLCs are incorporated into the optimization process in agreement to satisfy the defined objectives [20]. As the first number of iterations elapse, an ideal fluence distribution is determined iteratively, followed by a conversion from the fluence distribution into MLC segments. The optimization is carried out on the MLC positions directly [19]. Optimization with Direct S & S requires two actions: the fluence optimization and the final absorbed dose calculation [18]. The optimization can be repeated several times, with each repetition carried out with new adjusted objectives, to achieve a better result and eventually an optimal solution [19].

To be able to run the MLC segmentation in OMP, the maximum number of segments is specified together with the additional settings, as for example minimum allowed segment area and minimum number of open MLC leaves per segment. The segments not fulfilling these

requirements are rejected [18]. The process of creating segments is repeated with an adjusted number of initial fluence levels until the desired number of segments are accomplished [18]. The accurate absorbed dose calculation is undertaken as the objective function does not change much per iteration. This is exclusively performed in the first section of the specified stop criterion for the number of iterations [18]. The optimization continues from the current solution and subsequent iterations determine corrections to the fluence. As the stop criterion for the number of iterations has been reached, the final absorbed dose calculation is carried out with the PBC algorithm [18].

1.8 Gantry Angle Optimization (GAO)

In Eclipse, the GAO starts by generating the new angles. The goal is to find the optimal set and position of angles [16]. This is performed, in accordance to the fluence optimization, by iteratively optimizing the beam angles to satisfy the set of user defined DVOs. The GAO in Eclipse is divided into two steps: global and local optimization. The global optimization creates new coplanar or non-coplanar field geometries [16]. It originates from a set of uniformly distributed beams to successively reach the number of beams that best fulfils the defined objectives. The number of fields is then decreased by an iterative ranking that excludes the number of fields of least relative importance. The local optimization commences as the global optimization stops. This optimization only tries combinations of gantry angles and do not change the number of fields. The local optimization can run without first running the global optimization. However, the most profitable results from GAO are achieved by running both the global and the local optimization [16].

Only local optimization is available in OMP [18]. This means that the GAO proceeds from the originally beam geometry i.e. those angles used for the fluence optimization with the procedure of the equidistant beam geometry. Though, the aim is still to receive a treatment plan with more beneficial gantry angels with regard to the importance of the defined objectives, compared to the beam geometry with equally spaced beams. The gantry angles are updated during the optimization to improve the plan [19, 20]. When the gantry angles are optimized, an approximate dose calculation is used to reduce the time needed [18]. Therefore it is advocated to run the optimization process twice and in the latter process without selecting the angle optimization option. The new gantry angles are generated from the first optimization as the second optimization process is performed and the final absorbed dose is calculated, in agreement with that of the fluence optimization in OMP, by using beam lets [18]. The final dose calculation for GAO in Eclipse and OMP is again applying the PBC algorithm [16, 18].

1.9 Trade-offs

The parotid glands represent the comprehensive organ for the salivary production [21] and the most prevalent late side effect after receiving radiation in the H & N region is total mouth dryness i.e. *Xerostomia* [22]. A comparison between conventional radiotherapy techniques and IMRT has proved a significantly higher incidence of Xerostomia for those patients treated with conventional radiotherapy [23]. By exploring the relationships between dose distributions in the parotid glands and the preservation of the salivary flow after radiation therapy, a dose threshold for Xerostomia might be investigated. Such a study has been performed by Eisbruch et al. [24] where an average absorbed dose threshold of 26 Gy (for the ipsilateral parotid gland) and 24 Gy (for the contra lateral parotid gland) was found. The dose threshold for the ipsilateral gland is also what is recommended as dose threshold for the parotid glands in the clinical dose protocol, DAHANCA [25].

As the inverse dose planning is a compromise in accomplishing the desired prescribed absorbed dose to the PTV and reducing high absorbed doses to the normal structures [5, 6 and 8], it is of interest to investigate this trade-off. Focusing on H & N cancer, a common situation

is that at least one of the parotid glands overlaps with at least one of the PTVs. In a clinical investigation [26] the trade-off between parotid gland sparing and the under-dosage to the PTV has been studied. It is established that sparing of the parotid glands is strongly dependant of the objectives for the PTV. By allowing small volumes of the PTV with under-dosage, though fulfilling the ICRU criterion [4], the average absorbed dose to the parotid glands is reduced. These trials aimed to show the real trade-off between parotid gland sparing and under-dosages of the PTV. An important aspect is though that an under-dosage and prevailed cold-spots in a tumour sub volume can have devastating consequences [27].

1.10 Pareto evaluation

To fairly compare two TPSs, a comparison between the entire systems is desirable. Earlier attempts in trying to compare different TPSs and delivery techniques has shown to be dependant on the available equipment and fail to perform a thorough comparison [13]. Bohusung et al. [28] managed to perform a multi-centre comparison in an ESTRO project between IMRT TPSs by scoring data generated from DVHs from each TPS by optimizing on an anthropomorphic pelvic phantom. In another more clinical oriented study a comparison between conformal radiotherapy and IMRT was accomplished, again by scoring the data from the DVHs with the addition of using a biological model [14]. Other studies have made even more exhaustive attempts to evaluate treatment plans as for example Akpati et al. [29] that introduced a unified dosimetry index in trying to rank the treatment plans.

A mathematical concept in expressing a trade-off between mutually inconsistent objectives was introduced by the economist Vilfredo Pareto [30]. Hence, the concept has been incorporated with its founder as *Pareto optimality*. A Pareto optimal solution is equivalent with the fact that one objective cannot be improved without impairing at least one other objective.

Concerning the IMRT procedure, a Pareto front is similar to a database of plans that fulfils the inverse dose planning goals from which the most optimal plan can be detected [13, 31]. The most optimal plan is situated in the bend of the curve i.e. where the sparing of the OAR, chosen for the trade-off, is capital along with least under-dosage of the PTV (Figure 2). Further, the Pareto fronts allows an understanding of the trade-offs for individual treatment plans [32].

An unbiased comparison is desired to be able to compare different TPSs as well as different delivery techniques. Evaluation based on *Pareto optimality* allows exploration of the interaction between two contradictions such as the absorbed dose coverage of the PTV and maximum or average absorbed dose to an OAR and their mutual interaction (Figure 2).
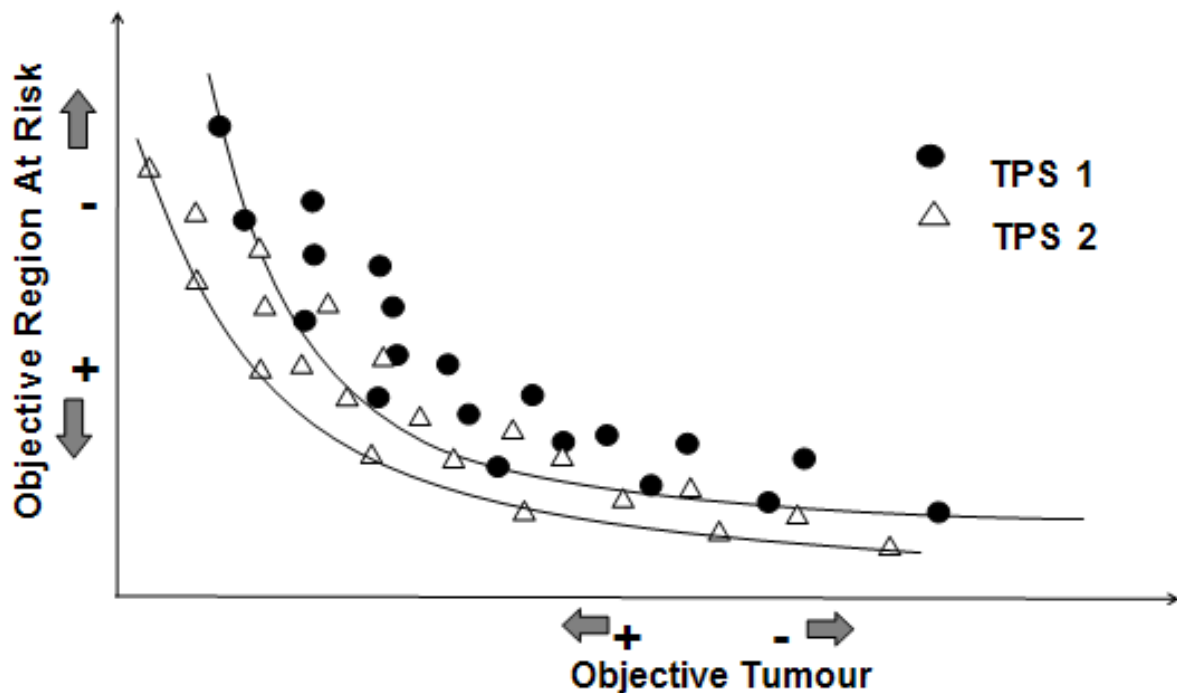
Figure 2. The Pareto optimality is illustrated by the dots and triangles situated on the two solid lines. The Pareto concept is applied to a typical IMRT situation: a contradiction between an objective to an OAR and an objective for the target. The plus sign denotes a more advantageous situation. Two TPSs are taken into account to visualize the possibility of distinguish between Pareto fronts from different TPSs.

A more optimal treatment plan than the one first generated may exist (Figure 2). Hence, by only comparing individual plans the comparison might be subjective. To avoid this fact, several treatment plans could be generated to represent one TPS. Craft and Bortfeld [33] inferred that N+1 treatment plans (where N is the number of objectives) is enough to sample a Pareto front. Rather than comparing individual treatment plans, a comparison between the Pareto fronts (Figure 2) may be employed as a potential tool when comparing different TPSs and delivery techniques and by that evading the fact of a subjective judgement. Furthermore, by exploring the interaction between the objectives, the operator receives the opportunity to choose the most clinically relevant compromise between the two contradictions [15, 32]. Considering a comparison based upon Pareto evaluation, one successful example is the comparison between IMRT and Intensity Modulated Proton Therapy (IMPT) by Steneker M et al. [34].

2. Material and methods

The initial work flow considers the inverse dose planning procedure in Eclipse and OMP. It should be pointed out that the dose planning in OMP was performed by another fellow Medical Physics student at Lund University Hospital. More specific optimization procedure follows afterwards and concerns Eclipse and OMP separately. It should be pointed out that this comparison was performed in the manner of enforcing a satisfactory coverage of the target and simultaneously maintain the regulations according to DAHANCA [25].

2.1 General work flow

The comparison between Eclipse and OMP was carried out as a "black box comparison" i.e. exclusively parameters were kept equal. Furthermore, the comparison was based upon three

different H & N cases: 1, 2 and 3. The cases were based on CT-data from three oropharynx cancer patients, previously treated at Lund University Hospital (Case 1) and Herlev University Hospital (case 2 and 3). Dose restrictions to all outlined structures were held according to what is stated in the DAHANCA protocol [25]. In this study, every high-lighted treatment plan met all the dose restrictions except for the parotid gland of interest. The maximum desired average absorbed dose to the parotid gland was, according to these regulations, 26 Gy with the end-point Xerostomia and the under-dosage to the PTV was defined as more than 1 % of the relative volume receiving less than 95 %, but more than 90 %, of the prescribed dose [25]. The tumours (T) were classified according to an established classification system [35]. This classification system has been updated to include absence/presence of disease in regional lymph nodes (N) and absence/presence of distal metastases (M) and is denoted as the TNM classification system [36].

The beam geometry was constituted of seven coplanar equidistant angles spread over 360° (0°, 51.4°, 102.9°, 154.3°, 205.7°, 257.1° and 308.6°) with the equidistant beam geometry and with those seven generated from GAO. The collimator angle was set to 2°. The dose per fraction was 2 Gy with a total absorbed dose of 68 Gy for the first case and 66 Gy in the remaining cases. If using a total absorbed dose of 68 Gy, the tumour extent is required to be 4 cm in some direction [25]. Photons with energy of 6 MV were used for all cases. Two linear accelerators were utilized: one at Lund University Hospital and one at Herlev University Hospital. The absorbed dose was calculated utilizing the PBC.

The average absorbed dose to the parotid gland in the trade-off was finally plotted as a function of the under-dosage to the PTV. The under-dosage and the average absorbed dose were received by extracted dosimetric data from the generated DVHs. These two parameters, for the equidistant beam geometry and GAO, constituted one dot in the Pareto space. However, treatment plans not fulfilling the clinical dose protocol, except for the overlapping parotid gland, [25] were not considered. The number of treatment plans was likely to differ between the cases due to the complexity in each case. The sufficient number of treatment plans to sample a Pareto front was seldom N+1 (where N denotes the number of objectives) as has been stated by Craft and Bortfeld [33].

2.2 IMRT inverse dose planning

2.2.1 Eclipse

Initially, an objective function for the PTVs was introduced. The objectives for the parotid gland chosen for the trade-off were not yet applied. Though, this structure and other OARs were already partially regarded with the NTOP. The optimization was ceased as the objective function did not alter from iteration to iteration. Eventually, the LMC and the final absorbed dose calculation were accomplished.

The treatment plan described above constituted the original plan from which all the other plans were created. The plan was copied and the constraints for the PTVs were unmodified. An upper objective function to the right parotid gland that was involved in the trade-off was introduced. Additionally, what in Eclipse is entitled as, a spline [16] was applied for the parotid gland of interest. The spline consisted of five objectives with different volume criteria. In summary, six objectives were applied for the parotid gland of interest. The volume criteria were set in order to manoeuvre the parotid average absorbed dose by only altering the importance. The importance of the objectives for the parotid gland chosen for the trade-off was varied in a systematically procedure in the creation of new treatment plans. The objectives for the PTVs and the remaining OARs for every new treatment plan were identical to the objectives in the original plan. The importance denotes the criteria for the DVOs that are regarded when computing the modulated field fluences that are converted into deliverable

DMLC sequences [16]. Hence, all DVOs are weighted together and composite one objective function that is minimized during the optimization to gradually achieve a dose distribution similar to that of the specified and desired dose distribution [5].

2.2.2 OMP

In OMP Direct S & S was used. The optimization procedure in OMP began likewise that in Eclipse by the definition of upper and lower objectives for the PTV with the designated relative importance. Since OMP had no corresponding of the Eclipse NTOP, to *e.g.* suppress hot-spots in the normal tissues, all the normal tissues were included in the beginning. This was done by dedicating importance on their defined upper objectives. At this point the parotid gland of interest was given a low importance. As an optional mode, a subtraction between the outlined body part and the PTV was made in trying to mimic the Eclipse NTOP.

The optimization ran for a preset number of iterations. The maximum number of segments along with the minimum allowed segment area and minimum number of open MLC leaves per segment were adjusted before running the optimization. After receiving a satisfying coverage of the PTV, the relative importance of the parotid gland was modified. The importance to the remaining structures was unchanged.

2.3 Gantry Angle Optimization (GAO)

2.3.1 Eclipse

The original treatment plan settings, applied for the plans generated from the equidistant beam geometry, were used to generate treatment plans with GAO as well. The GAO was performed with the local and the global optimization procedure with the same objectives and relative importance as for the equally spaced beams. The most adequate angle combination, considering the importance of the objectives, was generated. The GAO started with a preset number of angles of seven which was the desired number. As the optimal angles were evoked, a new fluence optimization was carried out followed by the final absorbed dose calculation.

2.3.2 OMP

The GAO commenced by choosing the dedicated algorithm. All the treatment plans with seven equally spaced beams were re-optimized with GAO. In analogy with GAO in Eclipse, a standard optimization had to be performed with the new beam angles. Unlike Eclipse, OMP only used local GAO. The last step after GAO included the final absorbed dose calculation.

2.4 C*ase 1*

The first case that was used for the evaluation between Eclipse and OMP was based on CT-data from a patient diagnosed with oropharynx cancer (Figure 3). The prescribed dose was 68 Gy to PTV-T and 50 Gy to PTV-E. The tumour was defined as a T4 and the nodule spread was of N1 extent. This very first case represented a trade-off between the right parotid gland and PTV-T. PTV-E was just on the border of the right parotid gland and was therefore not taken into account in the trade-off. Case 1 included several different OARs apart from the right parotid gland: left and right lens, optic nerves, the front and the back of the eye, orbit and inner ear as well as the optic chiasm, brainstem, spinal cord, larynx and the left parotid gland.
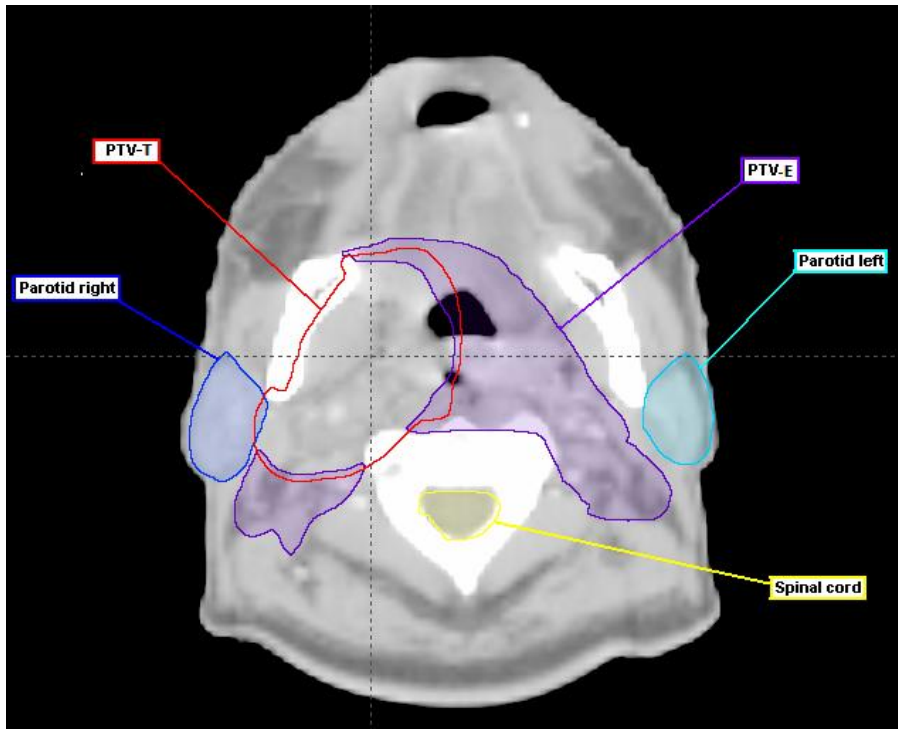
Figure 3. An original transverse CT-image section of case 1. The image high-lights the overlap between the right parotid gland and the PTV-T. Apart from the overlap, PTV-E, the left parotid gland and the spinal cord are showed as well.

2.5 Case 2

The second case was another oropharynx H & N cancer case, treated according to the DAHANCA protocol [25] with a prescribed dose of 66 Gy to the PTV-T. This case included several particular target structures with varying dose levels: PTV-T and PTV-N were supposed to receive 66 Gy, PTV-E 60 60 Gy and PTV-E 50 50 Gy. The tumour was defined as T2 and the nodule spread was of N1 extent. Optic chiasm and the right inner ear were also outlined. Since they were far away from to the trade-off region they were not included in the following illustration (Figure 4).
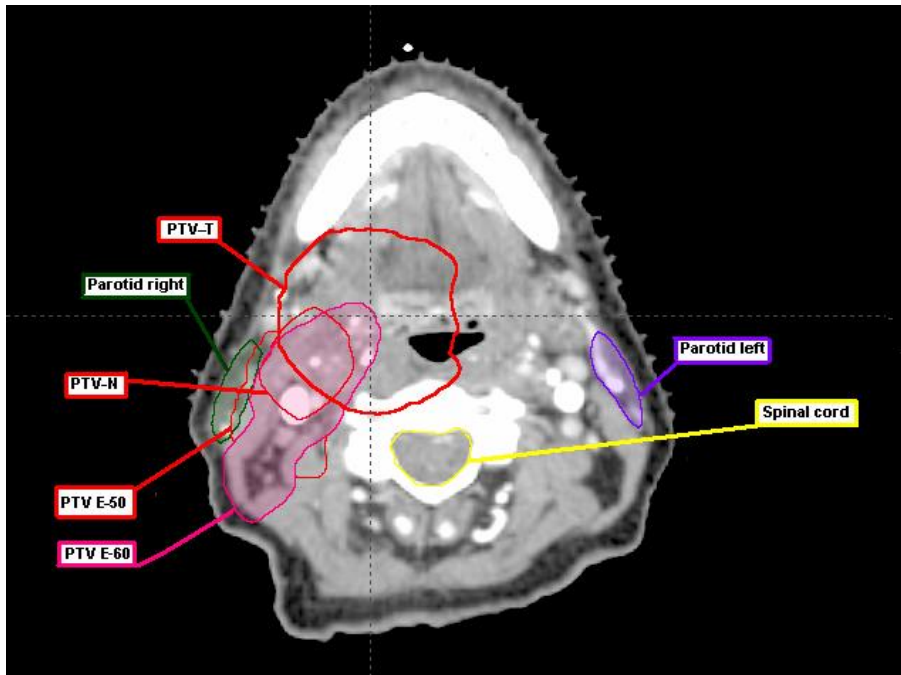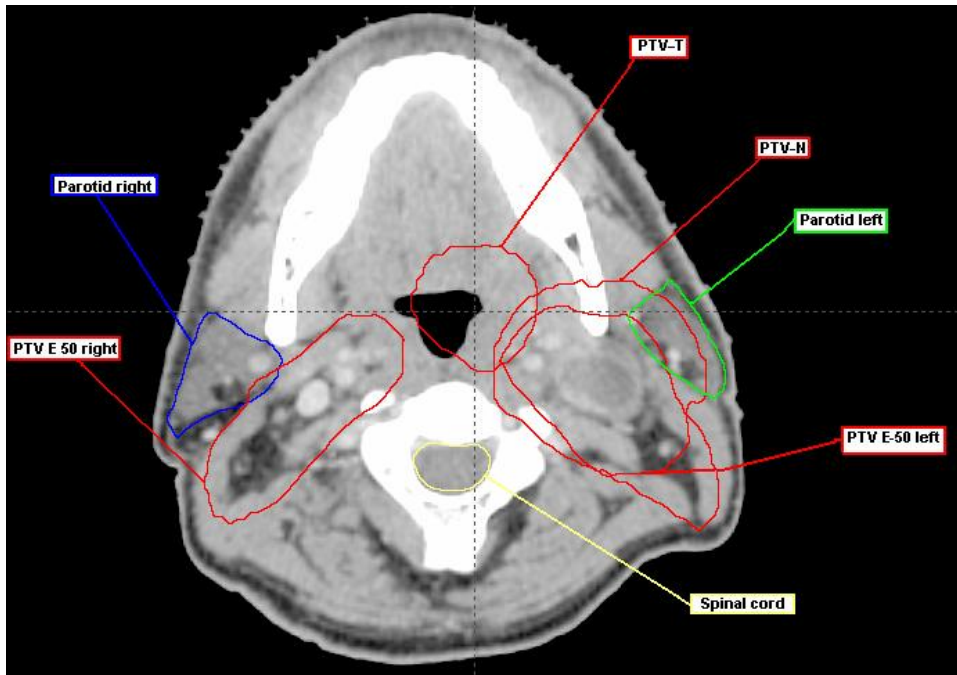
Figure 4. An original transverse CT-image section of the second H & N case, case 2. The image illustrates the overlap between the right parotid gland, PTV-T, PTV-E 50 and PTV-E 60. The PTV-N is also visible along with the spinal cord and the left parotid gland.

The trade-off in this case was between the right parotid gland and the target volumes; PTV-T, PTV-E 60 and PTV-E 50. The contour of PTV-N was just on the border of the right parotid gland. It was not necessary to put upper objectives on neither the left parotid gland nor the optic chiasm or the right inner ear since these structures already fulfilled the regulations according to DAHANCA [25] because of the geometry.

2.6 C*ase 3*

The third and also the last case used in the evaluation was, in analogy with case 2 diagnosed with oropharynx cancer with a prescribed dose to the PTV-T of 66 Gy (Figure 5) and treated with the DAHANCA regulations [25]. This case included several other PTVs: PTV-N which was supposed to receive 66 Gy as well and right and left PTV-E 50 that should be covered with 50 Gy each. The tumour was defined as T2 and the nodule spread was N2B.

The overlap and therefore also the trade-off was constituted mostly by the left parotid gland and the PTV-N and was hence taken into account in the optimization procedure. There was also an overlap, though minor, between the right parotid gland and the right PTV-E 50.

Figure 5. An original transverse CT-image section for case 3. Note the overlap between the left parotid gland, and PTV-N as well as the overlap between the same parotid gland and PTV E-50 left. The spinal cord, PTV-T and the overlap between the right parotid gland and the right PTV-E 50 are illustrated as well.

3. Results

3.1 Pareto fronts

3.1.1 *Case 1*

In the following figures, of the generated Pareto fronts, the average absorbed dose to the parotid gland of interest is plotted as a function of the under-dosage to the overlapping PTV.

The Pareto fronts that were produced from several treatment plans for case 1 are illustrated in Figure 6. The case is further described in *Material and methods* in section *2.4*.
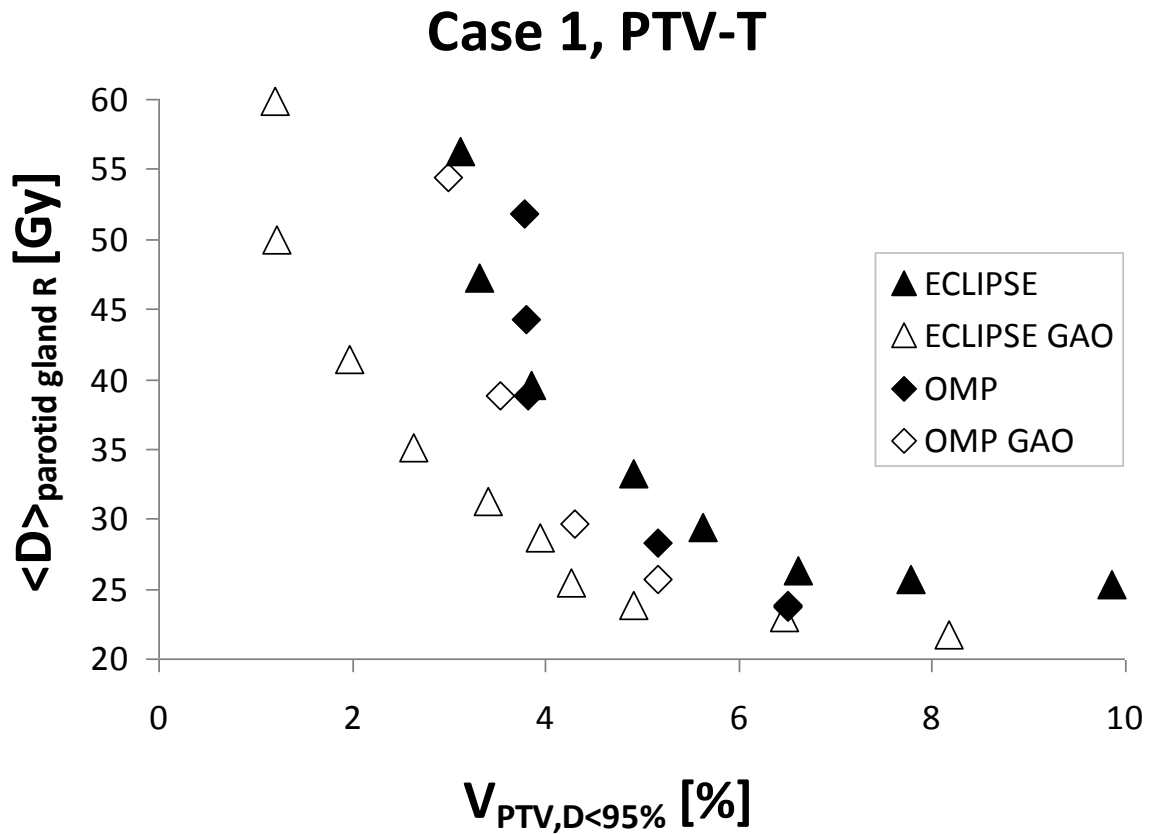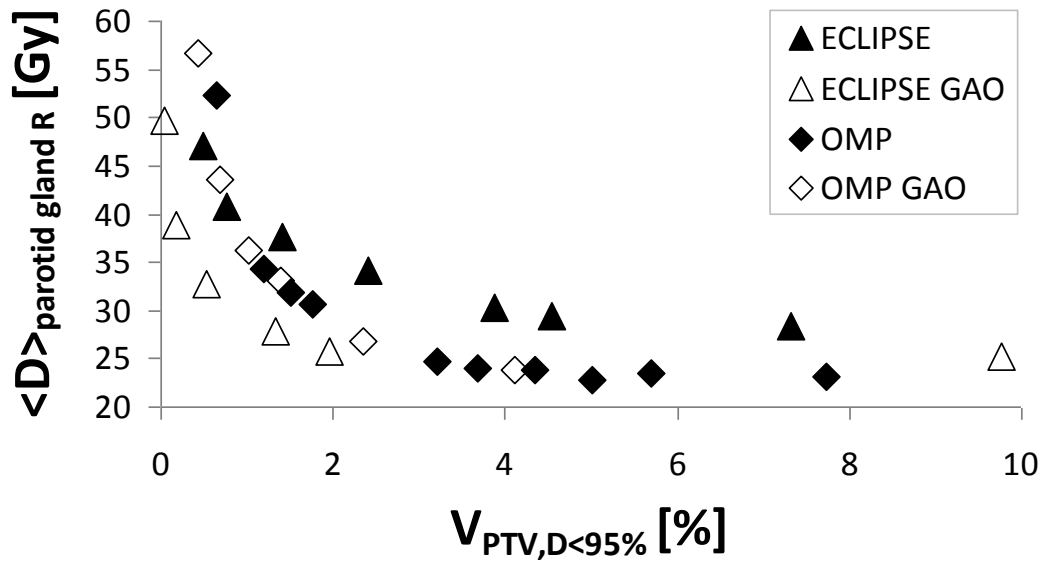
Figure 6. The figure illustrates the average absorbed dose to the right parotid gland as a function of the under-dosage to PTV-T for case 1 with equidistant beam geometry and GAO in Eclipse and OMP.

The figure above (Figure 6) indicates that every treatment plan followed the concept for a Pareto evaluation, i.e. coverage of the PTV-T decreased while improving sparing of the OAR chosen for the trade-off which i.e. the right parotid gland. The figure strengthens that it is possible to distinguish between Pareto fronts from different TPSs. It also visualizes the possibility to separate Pareto fronts with and without GAO.

3.1.2 *Case 2*

The Pareto fronts that were built out of numerous treatment plans for case 2 are visualized in Figure 7. The case is described more in detail in *Material and methods* in section *2.5*.
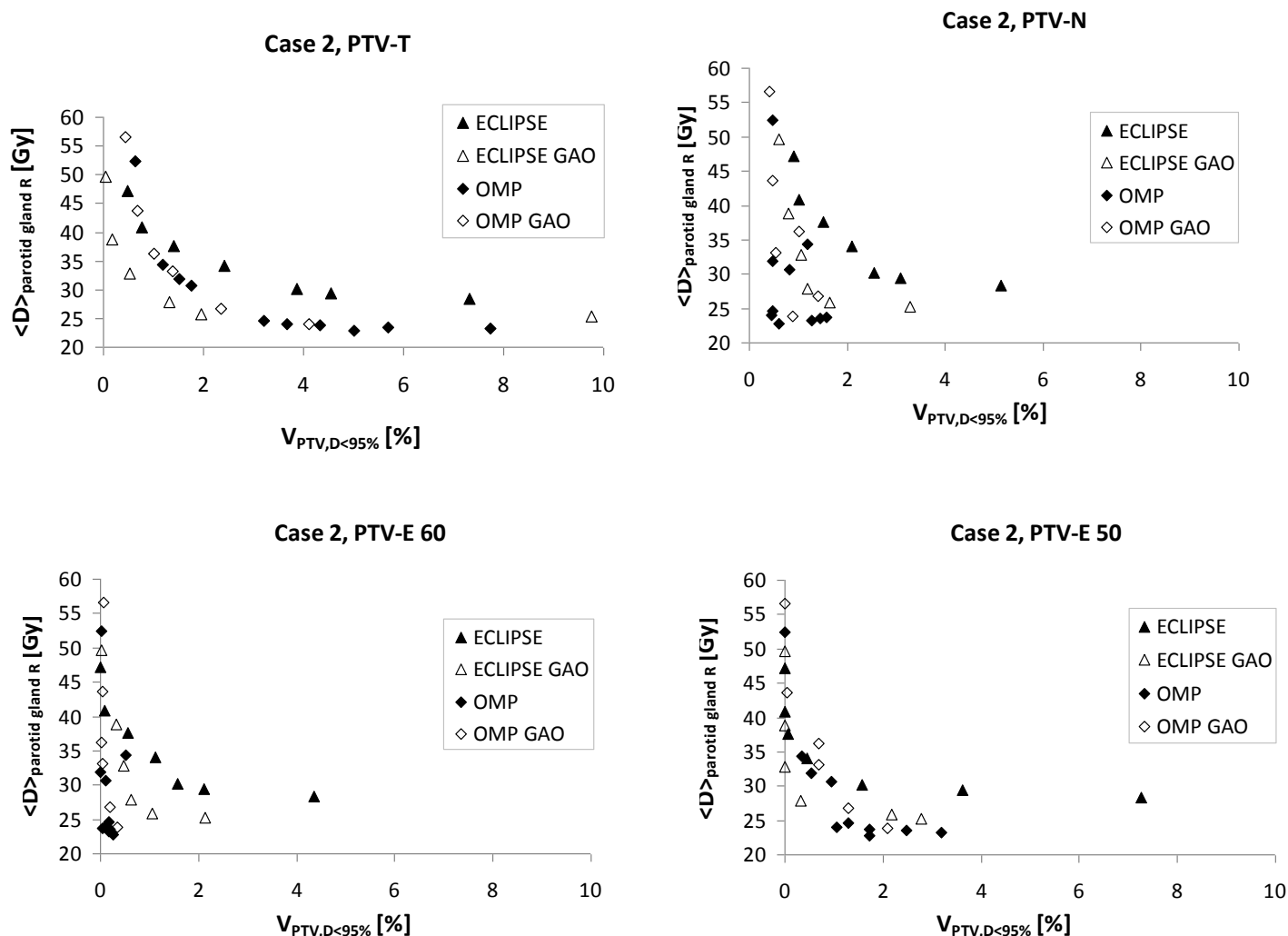
Case 2, PTV-T

Figure 7. The figure visualizes the average absorbed dose to the right parotid gland as a function of the under-dosage to the PTV-T for case 2 with equidistant beam geometry and GAO in Eclipse and OMP.

The illustration (Figure 7) indicates that all the treatment plans followed the concept for a Pareto evaluation i.e. coverage of the PTV-T again decreased while improving sparing of the right parotid gland. It also strengthens the possibility to discriminate between Pareto fronts generated from different TPSs and also elucidates that it is possible to separate Pareto fronts with and without GAO. The following plots (Figure 8) are the result of decreased coverage of the remaining PTVs (PTV-E 60, PTV-E 50 and PTV-N) while sparing of the right parotid gland is improving which indicate that the remaining PTVs follow the concept for a Pareto evaluation to a much lower extent (Figure 8).

Figure 8. The four plots above visualize the average absorbed dose to the right parotid gland as a function of the under-dosage to the PTV-E 60, PTV-E 50, PTV-T again and PTV-N for case 2 with equidistant beam geometry and GAO in Eclipse and OMP.

3.1.3 *Case 3*

The Pareto fronts for the last case, case 3, that were created from several treatment plans are elucidated in Figure 9. The fronts represent the trade-off between the left parotid gland and the under-dosage to PTV-N. This case was, in analogy with case 1 and 2, used for comparing OMP and Eclipse with equidistant beam geometry and GAO and is explained more in *Material and methods* in section *2.6*.
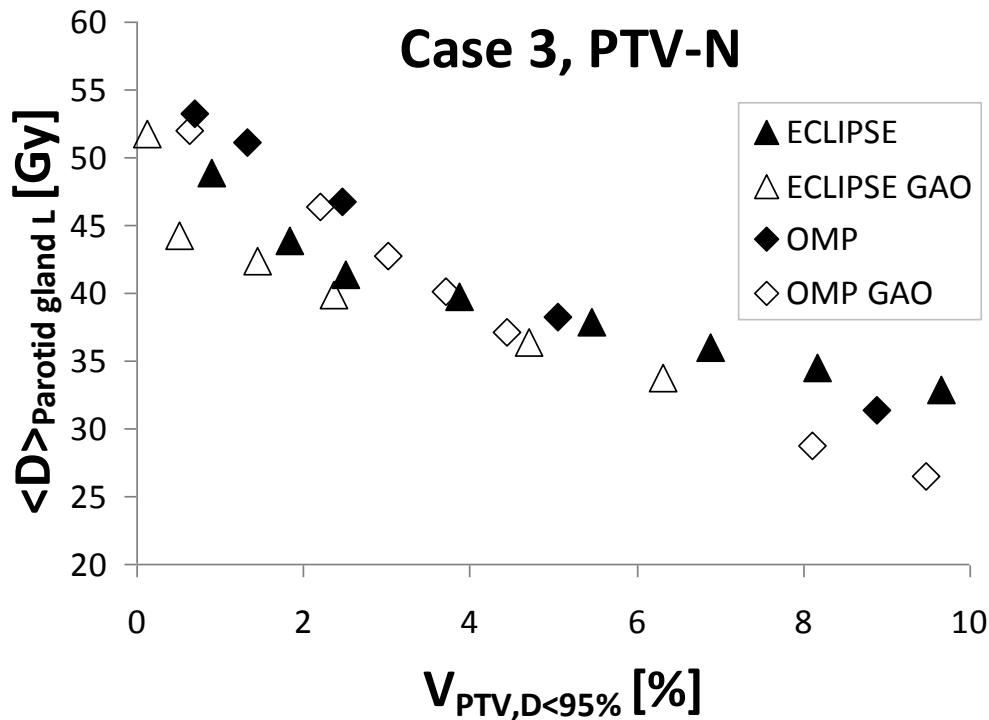
Figure 9. The figure illustrates the average absorbed dose to the left parotid gland as a function of the under-dosage to the PTV-N for case 3 with equidistant beam geometry and GAO in Eclipse and OMP.

In Figure 9 all treatment plans again seemed to follow the concept for a Pareto evaluation, i.e. coverage of the PTV-N decreased while improving sparing of the left parotid gland. The figure once again states that it is possible to distinguish between Pareto fronts from different TPSs and strengthen the possibility to separate Pareto fronts with and without GAO. Figure 10 includes the plots that are the effect of decreased coverage of the remaining PTVs (again PTV-N, PTV-E dx, PTV-E sin and PTV-T) while improving sparing of the left parotid gland. The majority of these PTVs did not follow the concept for a Pareto front evaluation.
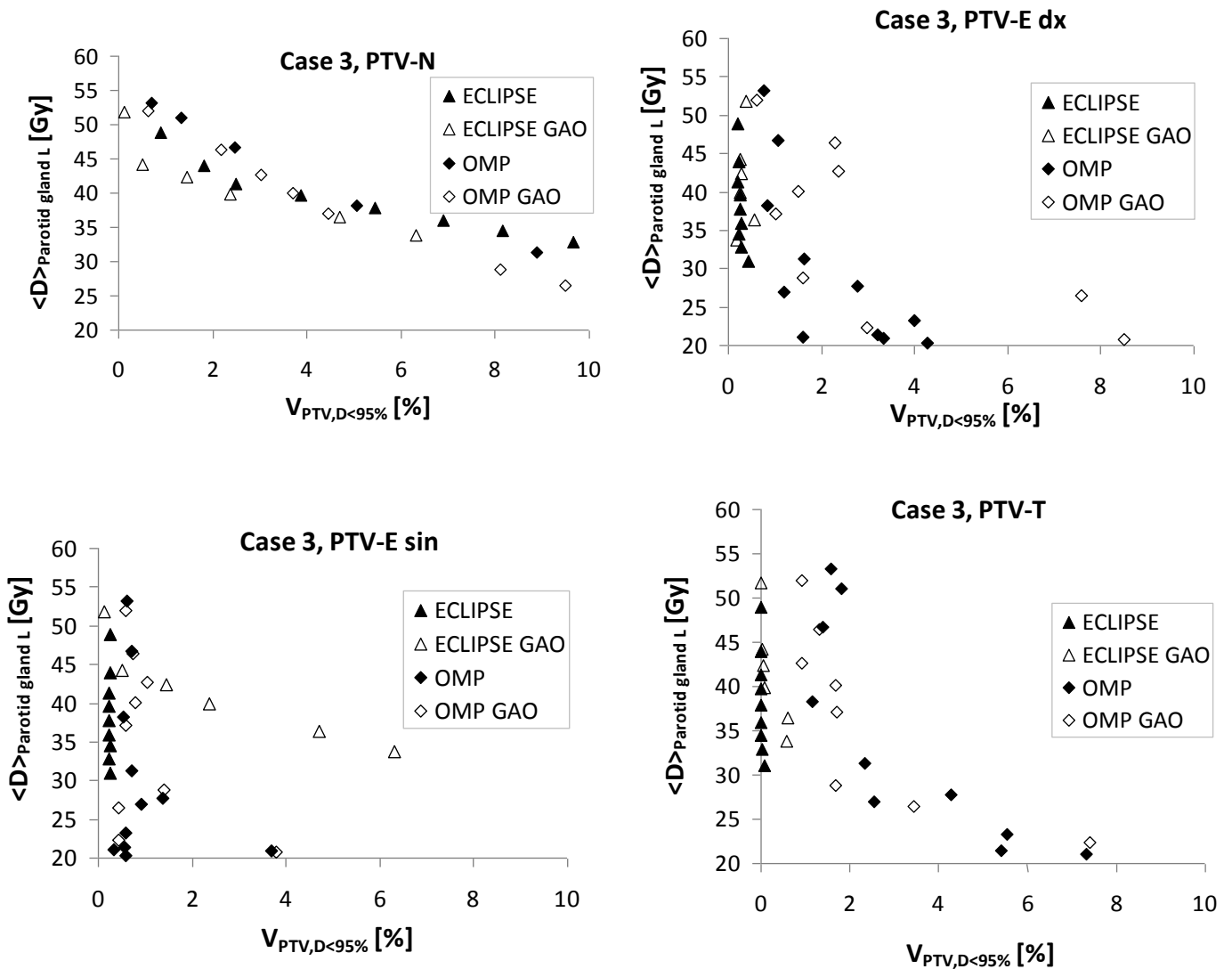
Figure 10. The figures visualize the average absorbed dose to the left parotid gland as a function of the under-dosage to the PTV-N again, PTV-E dx, PTV-E sin and PTV-T for case 3 with equidistant beam geometry and GAO in Eclipse and OMP.

3.2 Number of Monitor Units

Apart from the Pareto fronts, the number of monitor units (MUs) was studied for the dynamic (Eclipse) and the segmented (OMP) delivery technique separately. These are summarized in *Table 1-3*. The number of MUs is summarized as an average value for all the created treatment plans in each case. The tables visualize the number of MUs for each case for Eclipse and OMP with the equidistant beam geometry and GAO, as well as the decrease expressed in per cent, in number of MU using GAO.

Case 1		
MUs	**OMP**	**Eclipse**
Equidistant	629	1082

GAO	620	916
Decrease [%]	1.5	15.4

Table 1. The number of MUs for Eclipse and OMP for case 1 with the equally spaced beams and GAO together with the decrease, expressed in per cent, in number of MUs using GAO.

Case 2		
MUs	**OMP**	**Eclipse**
Equidistant	493	728
GAO	421	683
Decrease [%]	14.6	6.1

Table 2. The number of MUs for Eclipse and OMP for case 2 with the equally spaced beams and GAO together with the decrease, expressed in per cent, in number of MUs using GAO.

Case 3		
MUs	**OMP**	**Eclipse**
Equidistant	604	1083
GAO	566	775
Decrease [%]	6.3	28.4

Table 3. The number of MUs for Eclipse and OMP for case 3 with the equidistant beam geometry and GAO and the decrease, expressed in per cent, in number of MUs using GAO.

The tables above suggest that GAO lowers the number of MUs for both Eclipse and OMP for all treated cases. The number of MUs required to create a treatment plan was, in an analogy with what has been stated in earlier studies [10, 37], much fewer for the SMLC (OMP).

3.3 GAO, Beam Geometry

Since this Master's thesis primarily focused on comparison between different TPSs and different delivery techniques and mostly between equally spaced beams and GAO, the generated beam geometries for case 1-3 were studied in more detail. The beam geometries were represented by an average value of all of the treatment plans in every case for each TPS. Apart from the beam geometries generated from GAO, the equally spaced beams were included to be able to high-light the difference in the angle settings. The equidistant beam geometry (solid grey line), the beam geometry from OMP (dots) and the beam geometry from Eclipse (shaded lines) were applied to an original transverse CT-image (Figure 13).
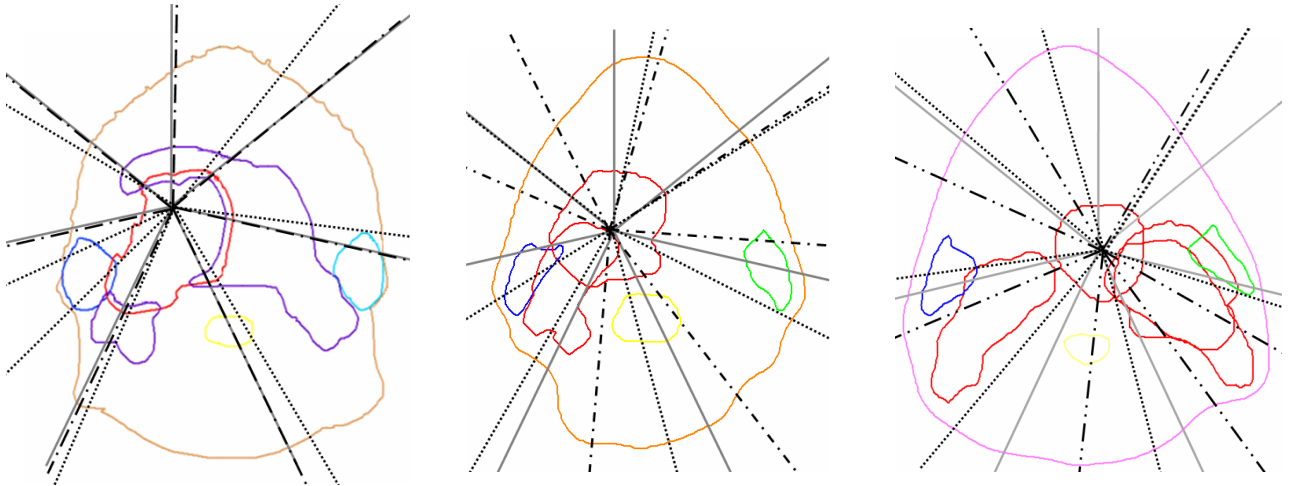
Figure 11. The figure indicates the different beam geometries generated from OMP (dots) and Eclipse (shaded line) along with the equidistant beam geometry (sold grey) for, from left to right, case 1, 2 and 3.

The beam geometries (Figure 11) imply that OMP and Eclipse generated different beam geometries. For example the beam geometry from Eclipse for case 2 avoids the right parotid gland to a higher extent than OMP. For case 3 it is stated that Eclipse increase sparing of the left parotid gland more than OMP since the beam setting again avoids placing beams on the gland in the trade-off. For case 1 only OMP differ from the equidistant angle settings.

4. Discussion

4.1. *Case 1*

This H & N case indicates the ability of distinguish between Pareto fronts from different TPSs with different delivery techniques and more particular between the GAO and equidistant beam geometry (Figure 6). The separation of the four Pareto fronts confirms that the systems studied are rather similar. Thus, the performance is improved considerably by using GAO.
What also is notable is that the Pareto fronts that originate from Eclipse are lower situated. This indicates that the Pareto fronts from Eclipse are more favourable since the dose coverage of the PTV is maintained to a higher extent as higher importance is applied to the right parotid gland. The most preferable front, comparing all the fronts, is the one generated using GAO in Eclipse.

The fronts originating from Eclipse seem to appear in a more structured pattern than those from OMP. Though, the under-dosage of the PTV is almost of the same extent for the Pareto fronts, except for the lower average absorbed dose to the right parotid gland which indicates a more favourable front.

The number of MUs is lowered while introducing GAO and the most obvious decrease is visible when utilizing GAO in Eclipse. Additionally, using GAO result in different beam geometries to that of the equidistant beam settings. This appearance is most legible for OMP. The decrease was around 2 % for OMP and 15 % for Eclipse. Further, the number of MUs demanded for creating a treatment plan was much fewer for SMLC (OMP) which is has been stated earlier by others [10, 37].

4.2. *Case 2*

Also case 2 (Figure 7) strengthens that it is possible to distinguish between Pareto fronts from different TPSs with different delivery techniques and more particular between GAO and

equally spaced beams. The systems studied are of rather similar character which is provided by the separation of the four Pareto fronts, thus utilizing GAO contributes to an ameliorated performance. The Pareto fronts that originate from GAO in Eclipse are more preferable than those from GAO in OMP since the dose coverage of the PTV is maintained to a higher extent as higher importance is applied to the right parotid gland. With equidistant beam geometry the same behaviour appears in the beginning of the fronts. Though, the bend of the Pareto front from OMP is situated more advantageous. Nevertheless, using GAO with Eclipse again results in the most adequate front. This case (Figure 7) is an example of a slight more complex case considering all the existing PTVs that are likely to have influence in the trade-off. Apart from the highlighted PTV (PTV-T), the remaining PTVs do not always follow the concept for a Pareto evaluation.

Besides the fact with more favourable fronts from GAO, the decrease in number of MUs is revealed: around 14 % for OMP and 6 % for Eclipse. Though, the necessary number of MUs for one treatment plan was much fewer for SMLC (OMP) which is a rather well known appearance [10, 37].

When comparing the beam geometries generated from GAO for Eclipse and OMP it is elucidated that the systems generate different beam geometries. In this case Eclipse appears to be the more advantageous TPS while considering the sparing of the right parotid gland.

4.3. *Case 3*

The results from the generated Pareto fronts (Figure 9) declare that also case 3 followed the concept for a Pareto evaluation and suggesting TPSs of rather similar character, even though GAO seems to be more advantageous. Likewise what did appear for the earlier cases and worth pointing out is that the Pareto fronts generated from GAO in Eclipse are more preferable than GAO in OMP. With equally spaced beams the same behaviour was observed in the beginning of the fronts. Though, the front from OMP is situated more desirable in the bend. The most preferable front, if comparing all the fronts, is again the one generated using GAO in Eclipse.

With this case Eclipse was having problems in accomplishing the desired clinical goal of an average absorbed dose to the left parotid gland of 26 Gy [25]. This could presumably be supplied with higher importance on the parotid gland. The current case (Figure 9) is a more complex case than both Case 1 (Figure 6) and Case 2 (Figure 7) since all the TPSs have difficulties in accomplishing a desirable average absorbed dose of 26 Gy [25] to the parotid gland of interest. This is also visualized by the steepness in the Pareto fronts (Figure 9). Though, due to the overlap and the existing hierarchy for the PTVs and OARs [25] one would not be able to spare this parotid gland clinically.

All the Pareto fronts for the PTVs (Figure 10) do not follow the concept for an evaluation grounded on the Pareto concept. It might depend on that they actually are affected by objectives on other adjacent structures as for example: the right PTV-E 50 is included in a trade-off between the right parotid gland.

In accordance with the results for case 1 and 2, the number of MUs for creating a treatment plan decrease by utilizing GAO. The decrease for OMP is about 6 % and for Eclipse around 28 %. The number of MUs demanded for creating a treatment plan is, in correspondence with what has been concluded before, much fewer for SMLC (OMP) [10, 36].

The TPSs produce different beam geometries. Again Eclipse is the most favourable system with the beam angle settings if regarding sparing of the left parotid gland. This advantage would probably be confirmed in a more convenient manner for Eclipse if higher importance is applied to the left parotid gland.

5. Conclusions

5.1. General conclusions

A comparison between different TPSs and different delivery techniques has appeared to be possible with a comparison represented by the Pareto front approach. Hence, Pareto evaluation is evidently a feasible comparison method. These findings correspond well to the aim of this study which partially was to compare two inverse TPSs.

Overall, the sparing of the parotid gland of interest can not be improved without target coverage being compromised. These two criteria represent two conflicting goals which is the investigating aim of the Pareto concept. The interaction between these criteria is thus highlighted by the entire database of all of the treatment plans i.e. the Pareto fronts.

Apparently the under-dosage is of quite same extent between the modalities for each specific case but with the difference of more sparing of the parotid gland in the trade-off which results in a superior Pareto front. The tendencies are expected to be the same if applying the Pareto concept to other cases where the trade-off concerns different sensitive structures. The treated cases represent different extent of complexity as visualized by both the steepness in the Pareto fronts and the difficulties in reaching a desirable average absorbed dose, without loosing target coverage, of 26 Gy to the parotid gland of interest [25].

The evaluation has verified that GAO contributes to plans with least under-dosage to the overlapping PTV together with the lowest absorbed dose to the parotid gland of interest i.e. the performance is improved by using GAO. The second part of the aim, i.e. to investigate IMRT with seven equally spaced beams with the most optimal seven gantry angles generated by using GAO, is also fulfilled. Besides, the GAO brings lowered number of MUs. Eclipse and OMP result in varied beam geometries when allowing them to generate seven gantry angles. The variations are of different character in the treated cases. A small difference from that of the equidistant beam geometry still results in a visible separation between the Pareto fronts.

5.2. Future aspects

For further investigation when comparing between different TPSs and delivery techniques it is possible to study the amount of sparing of sensitive structures in the previous trade-offs and in what extent it is done. It would also be interesting to focus on other end-points apart from Xerostomia which was studied in the current cases. The amount of sparing together with various end-points could possibly be studied by including biological models. One such model is the EUD-based model proposed by Niemierko et al. [38] that suggest a tool to be able to calculate the NTCP, and the TCP as well, for a particular treatment plan. The Pareto concept along with more specific data concerning the NTCP for the parotid gland and the TCP for the tumour might be promising in the development of the comparison.

In addition, the Pareto approach may also be applied for the same accelerators along with, for example, the implementation of one TPS's beam geometry into another to reduce the number of degrees of freedom. This idea can be strengthen by a study by V Marchesi et al. [9] where the modulation of SMLC and DMLC for the same accelerator was examined.

Similar cases with equal anatomy overlap and number of OARs could be used to study the reproducibility. Hence, different type of cases may be of more interest to illustrate the broadness in the comparison. In conclusion, more cases are demanded to confirm the findings in this Thesis. The broadness in the comparison may also be favoured by implementing other OARs in the trade-off. This could be performed to evaluate the assumption of similar tendencies between the Pareto fronts. In this first comparison this was not yet done since generating only one Pareto front is extremely time-consuming.

6. Acknowledgements

7. References

[1] American Cancer Society, Global Cancer Facts & Figures 2007, *Estimated Number of New Cancer Cases by World Area*, Legal Department of the American Cancer Society, 250 Williams St., NW, Atlanta, GA 30303-1002, pp.1-7, 2007

[2] www.socialstyrelsen.se, Socialstyrelsens statistikdatabas, dödsorsaksstatistik, antal döda

[3] Delaney G et al. *The role of radiotherapy in cancer treatment: Estimating optimal utilization from a review of evidence-based clinical guidelines*, Collaboration for Cancer Outcomes Research and Evaluation (CCORE), Liverpool Hospital, Sydney, Australia, Vol.107, No. 3, pp.660, 2006

[4] Griem L. M, *Prescribing, recording and reporting photon beam therapy by International Commission on Radiation Units and Measurements (ICRU)*, ICRU Report 50, Division of Radiation Biophysics Department of Radiation Oncology Massachusetts General Hospital Boston, MA 02114, Radiation research, Vol.138, No.1, pp.146-147, 1994

[5] Metcalfe P et al. *The physics of radiotherapy X-rays and electrons*, Medicals physics publishing, Madison Wisconsin, pp.472-492, 2007

[6] Hall J et al. *Radiobiology for the radiologist 6th edition,* Lippincott Williams & Wilkins, Philadelphia, 2006, pp.303-304

[7] Brahme A et al. *Optimization of stationary and moving beam radiation therapy techniques,* Department of Radiation Physics, The Karolinska Institute and University of Stockholm, Box 60204. S-104 01 Stockholm, Radiotherapy and Oncology, Vol.12, No.2, pp. 129-140, 1988

[8] Intensity Modulated Radiation Therapy Collaborative Working Group, *Intensity-modulated radiotherapy: current status and issues of interest,* International Journal of radiation Oncology*Biology*Physics, Vol.51, No. 4, pp.880-914, 2001

[9] V Marchesi et al. abstract in English: *Comparative dosimetry study of two methods of intensity modulation performed on the same accelerator,* Unité de radiophysique, CRLCC Alexis-Vautrin, avenue de Bourgogne, 54511 Vandoeuvre-lès-Nancy cedex, France, Cancer/Radiotherapy, Vol. 4, No.6, pp. 443-454, 2000

[10] Chui C.S et al. *Delivery of intensity-modulated radiation therapy with a multileaf collimator: comparison of step-and-shoot and dynamic leaf motion methods*, Department of Medical Physics, Memorial Sloan-Kettering Cancer Center, New York, NY 1002 1 USA Engineering in Medicine and Biology Society, 2000: Proceedings of the 22nd Annual International Conference of the IEEE , Vol.1, pp.460-462, 2000

[11] Porceddu S et al. *Radiation Oncology Intensity-modulated radiotherapy: Examples of its utility in head and neck cancer,* Division of Radiation Oncology, Peter MacCallum Cancer Centre, Melbourne, Australia, Australasian Radiology, Vol. 48, No.1, pp 51–57, 2004

[12] Ding M et al. *Dosimetric comparison between 3DCRT and IMRT Using Different Multileaf Collimators in the Treatment of Brain Tumours,* Radiation Oncology Department, University of Colorado Heath Science Centre, Aurora, CO, Medical Dosimetry, Vol. 34, No. 1, pp. 1-8, 2009

[13] Jatinder R. Palta and Rockwell M. T, *Intensity-Modulated Radiation Therapy, The State of the Art,* American association of Physicists in Medicine, Medical Physics Publishing, Madison, Wisconsin, 2003

[14] Cozzi L et al. *Three dimensional conformal vs. Intensity-modulated radiotherapy in head-and-neck cancer patients: comparative analysis of dosimetric and technical parameters*, pp.7-9, Medical physics unit, oncology institute of southern Switzerland, Bellinzona, Switzerland, Vol.58, No.2, pp.617-624, 2004

[15] Thieke C et al. *A new concept for interactive radiotherapy planning with multicriteria optimization: first clincal evaluation*, Department of Radiation Oncology, Deutches Krebsforschungszentrum, Heidelberg, Germany, Vol. 85, No.2, pp.292.-298, 2007

[16] Varian Medical systems, *Eclipse IMRT external beam planning system version 8.5.0*, Copyright © 2008

[17] Kamath S et al. *Algorithms for optimal sequencing of dynamic multileaf collimators,* Department of Computer and Information Science and Engineering, University of Florida, Gainesville, FL, USA, Phys. Med. Biol, Vol. 49, No.1, pp. 33–54, 2004

[18] Nucletron, Oncentra® MasterPlan v.3.1 SP3, *Physics and Algorithms*

[19] Nucletron, Oncentra® MasterPlan v3.1 SP3, *Help*

[20] Nucletron, Oncentra® MasterPlan v3.1 SP3, *User Manual*

[21] Cooper J.S et al. *Late effects of radiation therapy in the head and neck region,* NYU Medical Centre, New York, NY, International Journal of Radiation Oncology*Biology*Physics, Vol.67, No.31, pp.1141-1164, 1995

[22] Harrison LB et al. *Detailed quality of life assessment in patients treated with primary radiotherapy for cancer of the base of the tongue,* Brachytherapy Service, Department of Radiation Oncology, The Memorial Sloan-Kettering Cancer Centre, 1275 York Avenue, New York, New York 10021, John Wiley & Sons, Inc. Head Neck, Vol.19, No.3, pp.169-175, 1997

[23] Chao C K. S et al. *Protection of Salivary Function by Intensity-Modulated Radiation Therapy in Patients With Head and Neck Cancer,* Radiation Oncology Centre, Washington University, School of Medicine, St Louis, MO Seminars in Radiation Oncology, Vol. 12, No 1, pp. 20-25, 2002

[24] Eisbruch A et al. *Dose, volume, and function relationships in parotid salivary glands following conformal and intensity-modulated irradiation of head and neck cancer - The critical volume model,* Departments of *Radiation Oncology, Pathology, and Oncology, University of Michigan, Ann Arbor, MI, International Journal of Radiation Oncology*Biology*Physics, Vol.*45, No.3, pp.577-587, 1999*

[25] http://www.dahanca.dk/get_media_file.php?mediaid=57, DAHANCA 2004 Retningsliner for strålbehandling af hoved-hals cancer (Cavum Oris, Pharynx, Larynx) inklusiv IMRT vejledning

[26] Wilhelmius J.M DE Kruijf et al. *Quantification of the trade-off between parotid gland sparing and planning target volume under dosages in clinically node-negative head-and neck intensity modulated radiotherapy,* Department of Radiation Oncology, Erasmus MC-Daniël den Hoed, Rotterdam, The Netherlands, International Journal of Radiation Oncology*Biology*Physics, Vol.68, No.1, pp.136-143, 2007

[27] Tomé WA et al. *On cold spots in tumour sub volumes*, Department of Human oncology, University of Wisconsin Medical School, Madison, Wisconsin, Med Phys, Vol.29, No. 7, pp.1590-1598, 2002

[28] Bohsung J et al. ESTRO project, *IMRT Treatment planning: A comparative inter-system and inter-centre planning exercise of the QUASIMODO group,* Department of Radiotherapy, Charité Campus Mitte, Berlin, Germany, Vol.76, No.3, pp.354-361, 2005

[29] Akpati H et al. *Unified dosimetry index (UDI): a figure of merit for ranking treatment plans,* Department of Radiation Oncology, Stony Brook University School of Medicine, Stony Brook New York, U.S.A, Journal of Applied Clinical Medical Physics, Vol.9, No.3, Summer 2008

[30] Pareto V, *Cours d'Économie Politique,* F.Pichou, Lausanne and Paris, Vol.2, 1897

[31] Hong T.S et al. *Multicriteria Optimization in Intensity-Modulated Radiation Therapy Treatment Planning for Locally Advanced Cancer of the Pancreatic Head,* International Journal of Radiation Oncology*Biology*Physics, Vol. 72, No.4, 2008

[32] Craft D et al. *Exploration of tradeoffs in intensity-modulated radiotherapy*, Department of Radiation Oncology, Massachusetts General Hospital and Harvard Medical School, Boston, MA02114, Vol.50, No.24, pp.5857-5868, 2005

[33] Craft D and Bortfeld T, *How many treatment plans are needed in an IMRT multi objective plan database?* Department of Radiation Oncology, Massachusetts General Hospital and Harvard Medical School, Boston, MA 02114, USA, Phys Med Biol, Vol.53, pp.2785-2796, 2008

[34] Steneker M et al. *Intensity modulated photon and proton therapy for the treatment of head and neck tumours*, Department of Radiation Medicine, Paul Scherrer Institute, Villigen, Switzerland, Radiation and Oncology, Vol. 80, No.2, pp.263-267, 2006

[35] Hermanek P and Sobin LH, *TNM classification of malignant tumours, 4th ed*. Ed. International Union Against Cancer (UICC), Berlin, Heidelberg, New York Springer Verlag, 1992

[36] Hermanek P, Hutter RVP, Sobin LH et al., *TNM Atlas. Illustrated guide to the TNM/pTNM Classification of Malignant Tumours*, Heidelberg:Springer-Verlag Berlin Heidelberg, 1997

[37] Alaei P et al. *Comparison of dynamic and step-and-shoot intensity-modulated radiation therapy planning and delivery,* University of Minnesota, Minneapolis, MN USA, Medical Dosimetry, Vol. 29, No. 1, pp. 1-6, 2004

[38] Niemierko A et al. *A free program for calculating EUD-based NTCP and TCP in external beam radiotherapy,* Department of Radiation Oncology, Massachusetts General Hospital, Boston, MA, USA, Physica Medica, Vol.23, No.3-4, pp.115-125, 2007